

Multimessenger astrophysics of compact stars with exotic cores

Armen Sedrakian

Frankfurt Institute for Advanced Studies
Institute for Theoretical Physics, Wroclaw University

ICNFP Kolymbari,
26 August



FIAS Frankfurt Institute
for Advanced Studies



Uniwersytet
Wrocławski

Plan of the talk:

- 1 Covariant density functionals
- 2 Astrophysical constraints
- 3 Hypernuclear and hybrid compact stars
- 4 Bulk viscosity

In collaboration with:

[Mark Alford](#) (Washington University, St. Louis)

[Arus Harutyunyan](#) (Byurakan Astro. Observatory, Armenia)

[Jia-Jie Li](#) (South Western University, Chongqing China)

[Peter Rau](#) (Institute for Nuclear Theory, Seattle)

[Friedlin Weber](#) (Cal. U. at San Diego)

Multimessenger
astrophysics of
compact stars
with exotic
cores

A Sedrakian

Current
astrophysical
constraints

Introduction
and motivation

Current
astrophysical
constraints

Hyperons and
Delta-
resonances

Equation of
state of dense
matter

Results

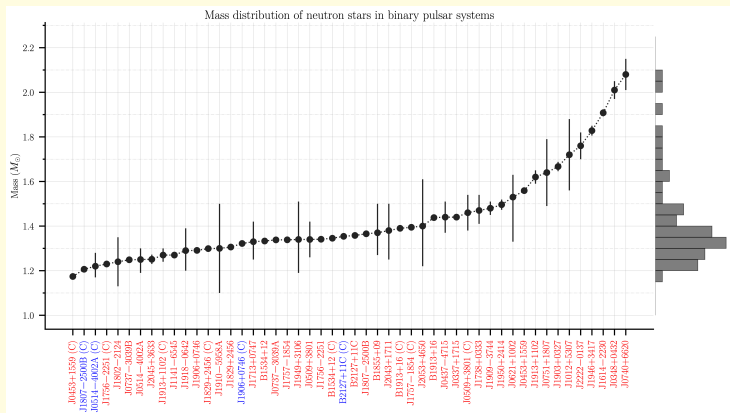
Bulk viscosity
from direct
Urca processes

Results

Conclusions-II

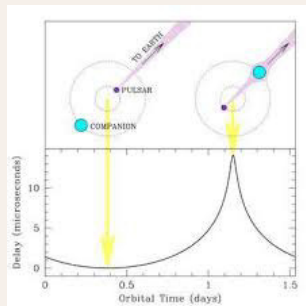
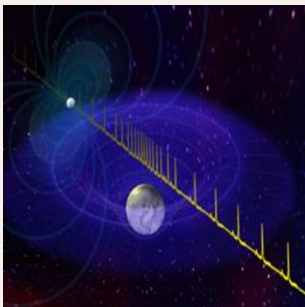
Astrophysical constraints

Pulsar mass measurements from radio observations



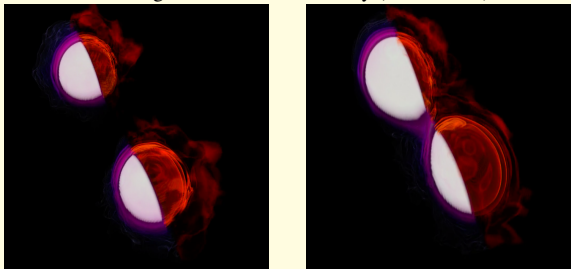
Credit: P. Freire, V. V. Krishnan, (MPIFR, Bonn).

Three two-solar-mass neutron stars in binaries with WD



- The millisecond pulsar J1614-2230 in a binary with a white dwarf, $M = 1.908 \pm 0.0164M_{\odot}$ (Demorest et al. 2010), **Relativistic Shapiro delay**.
- The millisecond pulsar J0348+0432 in a binary with a white dwarf $M = 2.01 \pm 0.04M_{\odot}$ (Antoniadis et al. 2013) [**theor. assumptions about WD cooling.**]
- The millisecond pulsar J0740+6620 $M = 2.14^{+0.10}_{-0.09}M_{\odot}$ (NANOGrav, Cromartie et al. 2019) **Relativistic Shapiro delay**.

Pre-merger deformation of binary (simulations)



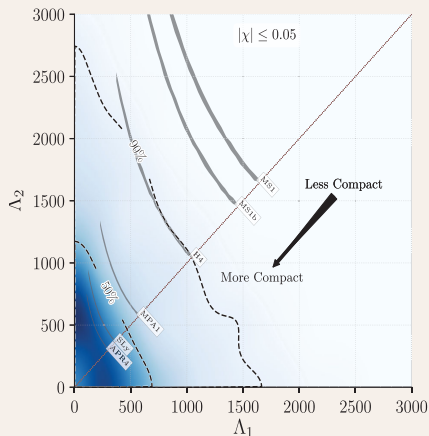
The gravitational wave signal allows for the extraction of the tidal deformability

$$Q_{ij} = -\lambda \mathcal{E}_{ij}, \quad \Lambda = \frac{\lambda}{M^5},$$

where Q_{ij} is the induced quadrupole moment, \mathcal{E}_{ij} is the tidal field of the partner, Λ is dimensionless tidal deformability.

TABLE I. Source properties for GW170817: we give ranges encompassing the 90% credible intervals for different assumptions of the waveform model to bound systematic uncertainty. The mass values are quoted in the frame of the source, accounting for uncertainty in the source redshift.

	Low-spin priors ($ \chi \leq 0.05$)	High-spin priors ($ \chi \leq 0.89$)
Primary mass m_1	1.36–1.60 M_\odot	1.36–2.26 M_\odot
Secondary mass m_2	1.17–1.36 M_\odot	0.86–1.36 M_\odot
Chirp mass \mathcal{M}	1.188 $^{+0.004}M$	1.188 $^{+0.004}M$



Multimessenger
astrophysics of
compact stars
with exotic
cores

A Sedrakian

Current
astrophysical
constraints

Introduction
and motivation

Current
astrophysical
constraints

Hyperons and
Delta-
resonances

Equation of
state of dense
matter

Results

Bulk viscosity
from direct
Urca processes

Results

Conclusions-II

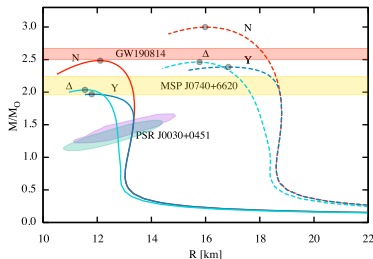
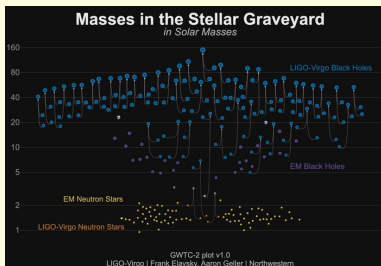
Mass gap objects

– **GW190814 event:** extreme mass asymmetric ratio created by a $22.2 - 24.3 M_{\odot}$ black hole and a $2.50 - 2.67 M_{\odot}$ compact object (no em counterpart).

The light (secondary) object's nature is enigmatic as it is in the mass gap $2.5 M_{\odot} \lesssim M \lesssim 5 M_{\odot}$.

– **GW230529 event:** The primary has mass $2.5 M_{\odot} \lesssim M \lesssim 4.5 M_{\odot}$

The secondary is a neutron star with mass in the range $1.2 M_{\odot} \lesssim M \lesssim 2.0 M_{\odot}$



Credit: LIGO-Virgo/Frank Elavsky/Northwestern

Solid curves – static solutions; dashed curves - maximally rotating (Keplerian) solutions from Sedrakian, Weber, Li Phys. Rev. D 102, 041301 (2020).

Multimessenger
astrophysics of
compact stars
with exotic
cores

A Sedrakian

Current
astrophysical
constraints

Introduction
and motivation

Current
astrophysical
constraints

Hyperons and
Delta-
resonances

Equation of
state of dense
matter

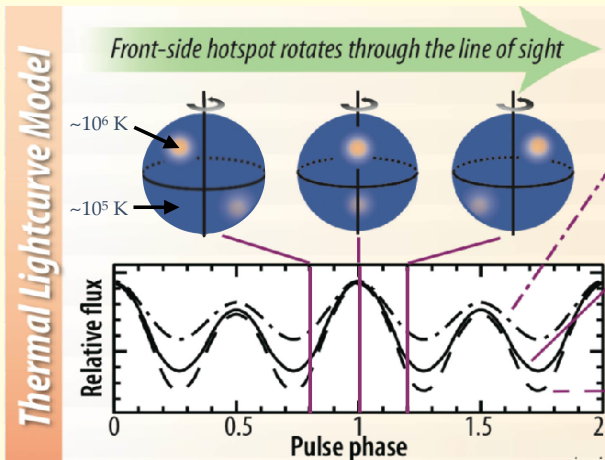
Results

Bulk viscosity
from direct
Urca processes

Results

Conclusions-II

Credit: NASA/NICER Mission Overview



Pulse-profile modeling of PSR J0030+0451 and PSR J0740+6620 [Riley et al 2019,2021],
Miller et al 2019,2021]

- $1.34_{-0.16}^{+0.15} M_{\odot} \rightarrow 12.71_{-1.19}^{+1.14}$ km, $1.44_{-0.14}^{+0.15} M_{\odot} \rightarrow 13.02_{-1.06}^{+1.24}$ km,
- $2.08_{-0.09}^{+0.09} M_{\odot} \rightarrow 12.39_{-0.98}^{+1.30}$ km, $2.07_{-0.07}^{+0.07} M_{\odot} \rightarrow 13.71_{-1.50}^{+2.61}$ km.

Multimessenger
astrophysics of
compact stars
with exotic
cores

A Sedrakian

Current
astrophysical
constraints

Introduction
and motivation

Current
astrophysical
constraints

Hyperons and
Delta-
resonances

Equation of
state of dense
matter

Results

Bulk viscosity
from direct
Urca processes

Results

Conclusions-II

Nuclear, hypernuclear, and delta-resonance matter

Nuclear and hypernuclear matter Lagrangian:

$$\begin{aligned}
 \mathcal{L}_{NM} = & \underbrace{\sum_B \bar{\psi}_B \left[\gamma^\mu \left(i\partial_\mu - g_{\omega BB} \omega_\mu - \frac{1}{2} g_{\rho BB} \boldsymbol{\tau} \cdot \boldsymbol{\rho}_\mu \right) - (m_B - g_{\sigma BB} \sigma) \right]}_{\text{baryons}} \psi_B \\
 & + \underbrace{\frac{1}{2} \partial^\mu \sigma \partial_\mu \sigma - \frac{1}{2} m_\sigma^2 \sigma^2 - \frac{1}{4} \omega^{\mu\nu} \omega_{\mu\nu} + \frac{1}{2} m_\omega^2 \omega^\mu \omega_\mu - \frac{1}{3} b m_B (g_\sigma \sigma)^3 - \frac{1}{4} c (g_\sigma \sigma)^4}_{\text{mesons}} \\
 & - \underbrace{\frac{1}{4} \boldsymbol{\rho}^{\mu\nu} \boldsymbol{\rho}_{\mu\nu} + \frac{1}{2} m_\rho^2 \boldsymbol{\rho}^\mu \cdot \boldsymbol{\rho}_\mu}_{\text{mesons}} + \underbrace{\sum_\lambda \bar{\psi}_\lambda (i\gamma^\mu \partial_\mu - m_\lambda) \psi_\lambda}_{\text{leptons}} - \underbrace{\frac{1}{4} F^{\mu\nu} F_{\mu\nu}}_{\text{electromagnetism}},
 \end{aligned}$$

- B -sum is over the baryonic octet
- Meson fields include scalar σ and vector ρ_μ -meson and ω_μ -mesons
- Leptons include electrons, muons and their neutrinos (for $T > 5$ MeV ν are trapped)

- Evaluate the partition function from the Lagrangian in the mean-field approximation and for infinite matter.
- At zero temperature this gives a functional of pressure versus energy-density $P(\varepsilon)$, at finite temperature $P(\varepsilon, T)$ or $P(\varepsilon, s)$, thus defines a density functional theory which is highly successful in condensed matter.

Merits and shortcomings:

- **Relativistic models of nuclear matter as DFT:**
 - (a) relativistic covariance, causality is fulfilled (+)
 - (b) The Lorentz structure of interactions is maintained explicitly (+)
 - (c) fast implementation (+)
 - (d) not a fundamental QFT (!), i.e., not part of the standard model (-)
 - (e) Viewed as a DFT with the parameters that are adjusted to the available data (astrophysics, laboratory, and ab initio calculations)
- **Easily extendable to finite-temperature**
Applicable to proto-neutron stars, binary neutron star mergers and supernovas within the same framework
- **Easily extendable to the strange sector and resonances**
Same-framework extensions to the strange sector incorporating experimental information from hypernuclei and astrophysical constraints

Two types of relativistic density functionals based on relativistic Lagrangians

- linear mesonic fields, density-dependent couplings (DDME2, DD2, etc.)
- non-linear mesonic fields; coupling constants are just numbers (NL3, GM1-3, etc.)

Fixing the couplings: nucleonic sector

$$g_{iN}(\rho_B) = g_{iN}(\rho_0)h_i(x), \quad h_i(x) = a_i \frac{1 + b_i(x + d_i)^2}{1 + c_i(x + d_i)^2} \quad i = \sigma, \omega,$$

$$g_{\rho N}(\rho_B) = g_{\rho N}(\rho_0) \exp[-a_\rho(x - 1)], \quad i = \rho, (\pi - HF)$$

Meson (i)	m_i (MeV)	a_i	b_i	c_i	d_i	g_{iN}
σ	550.1238	1.3881	1.0943	1.7057	0.4421	10.5396
ω	783	1.3892	0.9240	1.4620	0.4775	13.0189
ρ	763	0.5647				7.3672

$h_i(1) = 1$, $h_i''(0) = 0$ and $h_i''(1) = h_i''(1)$, which reduce the number of free parameters to three in this sector.

- DD-ME2 parametrization, G. Lalazissis, et al., Phys. Rev. **C71**, 024312 (2005), DD2 parametrizations, S. Typel, Eur. Phys. J. **A52**, 16 (2016)
- DD-ME2+LQ parametrizations, J. J. Li, Sedrakian, Phys. Rev. **C100**, 015809 (2019), ApJ 957:41 (2023).

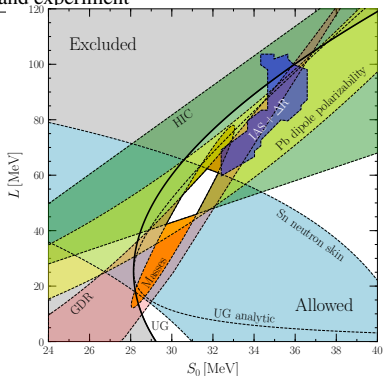
Taylor expansion of nuclear energy

$$E(\chi, \delta) \simeq E_0 + \frac{1}{2!} K_0 \chi^2 + \frac{1}{3!} Q_{\text{sat}} \chi^3 + E_{\text{sym}} \delta^2 + L \delta^2 \chi + \mathcal{O}(\chi^4, \chi^2 \delta^2), \quad (1)$$

where $\delta = (n_n - n_p)/(n_n + n_p)$ and $\chi = (\rho - \rho_0)/3\rho_0$.

Consistency between the density functional and experiment

- saturation density
 $\rho_0 = 0.152 \text{ fm}^{-3}$
- binding energy per nucleon
 $E/A = -16.14 \text{ MeV}$,
- incompressibility
 $K_{\text{sat}} = 251.15 \text{ MeV}$,
- skewness $Q_{\text{sat}} = 479$
- symmetry energy
 $E_{\text{sym}} = 32.30 \text{ MeV}$,
- symmetry energy slope
 $L_{\text{sym}} = 51.27 \text{ MeV}$,
- symmetry incompressibility
 $K_{\text{sym}} = -87.19 \text{ MeV}$



Credit: Tews, et al ApJ, 2017

New parametrizations of density functional [Li-Sedrakian, ApJ 957:41 (2023)]

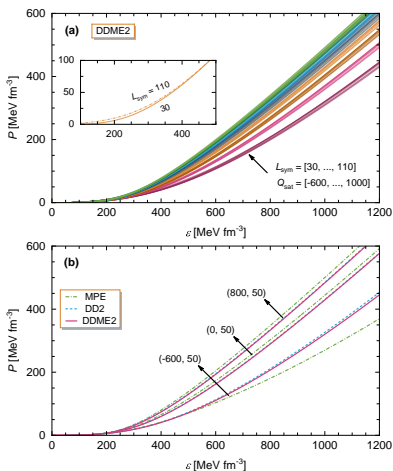
- Uncertainties are quantified in terms of variation of higher-order characteristics around the central fit values.
- Low density physics depends strongly on the value of L_{sym} with a strong correlation to the radius of the star and tidal deformability
- High-density physics strongly depends on the value of Q_{sat} with strong correlations to the mass of the star.

$$E(\chi, \delta) \simeq E_0 + \frac{1}{2!} K_0 \chi^2 + \frac{1}{3!} Q_{\text{sat}} \chi^3 + E_{\text{sym}} \delta^2 + L_{\text{sym}} \delta^2 \chi + \mathcal{O}(\chi^4, \chi^2 \delta^2), \quad (2)$$

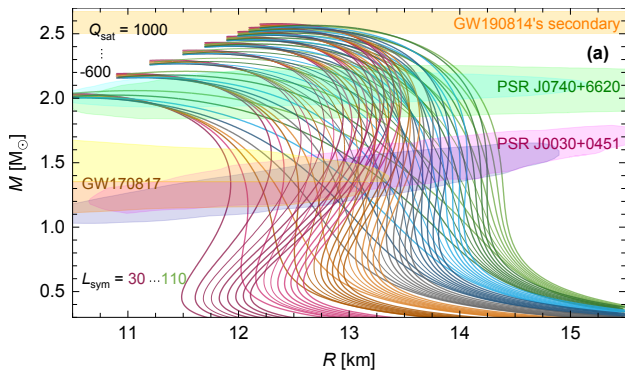
where $\delta = (n_n - n_p)/(n_n + n_p)$ and $\chi = (\rho - \rho_0)/3\rho_0$.

Generated a large number of EoS based on DDME2, DD2 and MPE functionals
($9 \times 9 = 81$ for each)

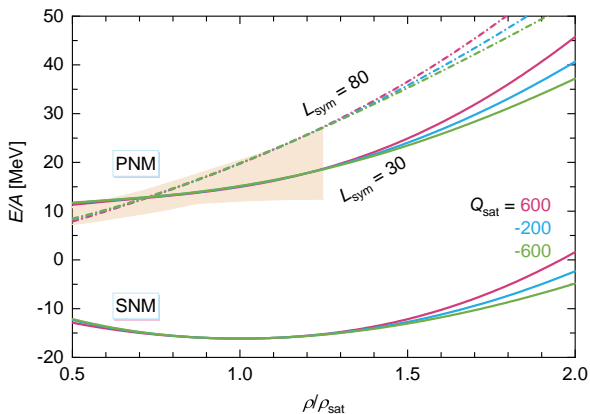
- skewness $-600 \leq Q \leq 1000$ MeV
- symmetry energy slope $30 \leq L_{\text{sym}} \leq 110$ MeV



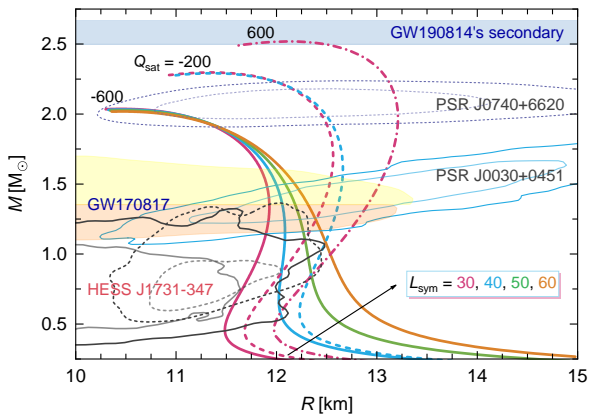
EoS for purely nucleonic stellar matter. In panel (a) the models are generated with DDME2 family of CDF models by varying the parameters $Q_{\text{sat}} \in [-600, 1000]$ MeV and $L_{\text{sym}} \in [30, 110]$ MeV. The effects of parameter L_{sym} on the low-density region of EoS are shown in the inset for illustration. In panel (b) the same is shown for three families of CDF models with fixed values of pairs $(Q_{\text{sat}}, L_{\text{sym}})$ (in MeV) as indicated in the plot.



Mass-radius relations for nucleonic EoS modes with different pairs of values of Q_{sat} and L_{sym} (in MeV). The color regions show the 90% CI ellipses from each of the two NICER modeling groups for PSR J0030+0451 and J0740+6620, the 90% CI regions for each of the two compact stars that merged in the gravitational wave event GW170817, and finally the 90% CI for the mass of the secondary component of GW190814.



Energy per particle of symmetric nucleonic matter (SNM) and pure neutron matter (PNM) as a function of density ρ/ρ_{sat} , obtained from six representative $(Q_{\text{sat}}, L_{\text{sym}})$ pairs (in MeV). The band corresponds to the combined χ EFT results from Huth et al. (2021). [Phys. Lett. B 844, 138062 (2023)]



$M - R$ relation for nucleonic EoS models with different pairs of values of Q_{sat} and L_{sym} . We show three branches of $M - R$ curves, for $Q_{\text{sat}} = -600$ (solid lines), -200 (dashed lines) and 600 MeV (dash-dotted lines). For each of these, L_{sym} is varied from 30 MeV to larger values that are still compatible with the ellipse of HESS J1731-347 at 95.4% CI. The shaded regions show the constraints from the analysis of GW events the ellipses indicate the regions compatible with the inferences from NICER observations, the contours show the $M - R$ constraints for the CCO in HESS J1731-347 Doroshenko (2022). [Phys. Lett. B 844, 138062 (2023)]

Multimessenger astrophysics of compact stars with exotic cores

A Sedrakian

Current astrophysical constraints

Introduction and motivation

Current astrophysical constraints

Hyperons and Delta-resonances

Equation of state of dense matter

Results

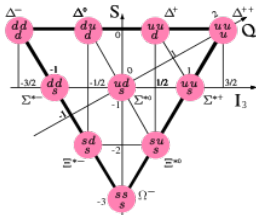
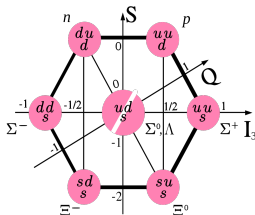
Bulk viscosity from direct Urca processes

Results

Conclusions-II

Beyond nucleons: Baryon octet $J^P = 1/2^+$ and baryon decuplet $J^P = 3/2^+$

Strangeness carrying baryons + resonances (nucleon excitations)



Hypernuclear matter Lagrangian:

$$\mathcal{L}_{NM} = \underbrace{\sum_B \bar{\psi}_B \left[\gamma^\mu \left(i\partial_\mu - g_{\omega BB} \omega_\mu - \frac{1}{2} g_{\rho BB} \boldsymbol{\tau} \cdot \boldsymbol{\rho}_\mu \right) - (m_B - g_{\sigma BB} \sigma) \right] \psi_B}_{\text{baryons}}$$

$$+ \underbrace{\frac{1}{2} \partial^\mu \sigma \partial_\mu \sigma - \frac{1}{2} m_\sigma^2 \sigma^2 - \frac{1}{4} \omega^{\mu\nu} \omega_{\mu\nu} + \frac{1}{2} m_\omega^2 \omega^\mu \omega_\mu - \frac{1}{3} b m_B (g_\sigma \sigma)^3 - \frac{1}{4} c (g_\sigma \sigma)^4}_{\text{mesons}}$$

$$- \underbrace{\frac{1}{4} \boldsymbol{\rho}^{\mu\nu} \boldsymbol{\rho}_{\mu\nu} + \frac{1}{2} m_\rho^2 \boldsymbol{\rho}^\mu \cdot \boldsymbol{\rho}_\mu}_{\text{mesons}} + \underbrace{\sum_\lambda \bar{\psi}_\lambda (i\gamma^\mu \partial_\mu - m_\lambda) \psi_\lambda}_{\text{leptons}} - \underbrace{\frac{1}{4} F^{\mu\nu} F_{\mu\nu}}_{\text{electromagnetism}}$$

$R_{\alpha Y} = g_{\alpha Y}/g_{\alpha N}$ and $\kappa_{\alpha Y} = f_{\alpha Y}/g_{\alpha Y}$ for hyperons in SU(6) spin-flavor model

$R \backslash Y$	Λ	Σ	Ξ
$R_{\sigma Y}$	2/3	2/3	1/3
$R_{\sigma^* Y}$	$-\sqrt{2}/3$	$-\sqrt{2}/3$	$-2\sqrt{2}/3$
$R_{\omega Y}$	2/3	2/3	1/3
$\kappa_{\omega Y}$	-1	$1 + 2\kappa_{\omega N}$	$-2 - \kappa_{\omega N}$
$R_{\phi Y}$	$-\sqrt{2}/3$	$-\sqrt{2}/3$	$-2\sqrt{2}/3$
$\kappa_{\phi Y}$	$2 + 3\kappa_{\omega N}$	$-2 - \kappa_{\omega N}$	$1 + 2\kappa_{\omega N}$
$R_{\rho Y}$	0	2	1
$\kappa_{\rho Y}$	0	$-3/5 + (2/5)\kappa_{\rho N}$	$-6/5 - (1/5)\kappa_{\rho N}$
$f_{\pi Y}$	0	$2\alpha_{ps}$	$-(1/2)\alpha_{ps}$

$\alpha_{ps} = 0.40$, κ is the ratio of the tensor to vector couplings of the vector mesons.

The depth of hyperonic potentials in the symmetric nuclear matter are used as a guide the range of hyperonic couplings:

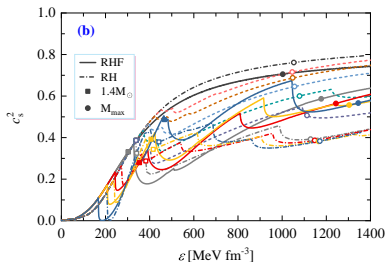
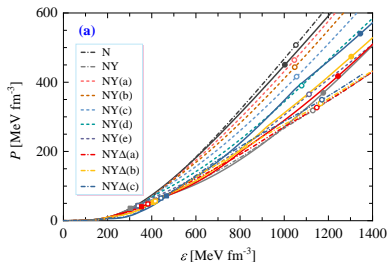
- Λ particle: $V_{\Lambda}^{(N)}(\rho_0) \simeq -30$ MeV
- Ξ particle: $V_{\Xi}^{(N)}(\rho_0) \simeq -14$ MeV
- Σ particle: $V_{\Sigma}^{(N)}(\rho_0) \simeq +30$ MeV

These ranges capture the most interesting regions of the parameter space of masses and radii.

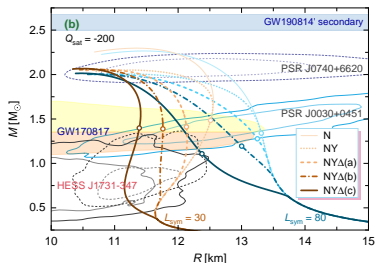
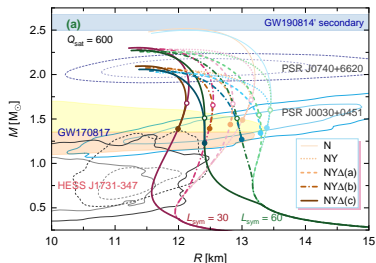
The depth of Δ -potentials in the symmetric nuclear matter is used as a guide for the range of the couplings:

- Electron and pion scattering: $-30 \text{ MeV} + V_{\Delta}^{(N)}(\rho_0) \leq V_{\Delta}(\rho_0) \leq V_N(\rho_0)$
- Use instead $R_{m\Delta} = g_{m\Delta}/g_{mN}$ for which the typical range used is

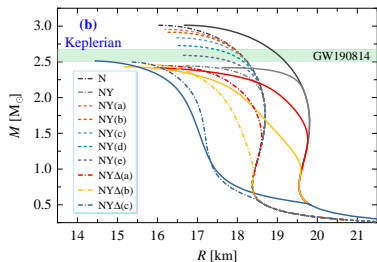
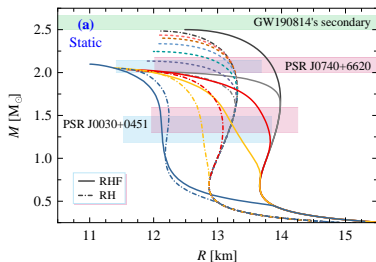
$$R_{\rho\Delta} = 1, \quad 0.8 \leq R_{\omega\Delta} \leq 1.6, \quad R_{\sigma\Delta} = R_{\omega\Delta} \pm 0.2.$$



EoSs for stellar matter featuring different compositions, i.e., nucleonic (N), hyperonic (NY), and hyperon- Δ admixed (NY Δ) one (panel a), and the associated speed of sound squared c_s^2 (panel b). The results are obtained using both the RHF and RH approaches. The positions for canonical-mass and maximum-mass configurations are marked by squares and circles.



$M - R$ relation for hyperon- Δ admixed EoS models for different Δ potential depths at nuclear saturation density $U_{\Delta}/U_N = 1, 4/3, 5/3$, which are labeled as “NY Δ (a-c)”, respectively. The results for purely nucleonic and hyperonic EoS models are also shown. In panel (a) the EoS models are constructed from the nucleonic model with pairs of $(Q_{\text{sat}}, L_{\text{sym}}) = (600, 30)$ and $(600, 60)$ MeV, combined with either SU(6) or a SU(3) symmetric model for the hyperonic sector. In panel (b) the EoS models are constructed from the nucleonic model with pairs of $(Q_{\text{sat}}, L_{\text{sym}}) = (-200, 30)$ and $(-200, 80)$ MeV and a SU(3) symmetric parametrization of the hyperonic sector. The onset mass of hyperons for each EoS model is marked by circles.



Mass-radius relations of CSs in the static and maximal fast rotating (Keplerian) limits for various EoS models. The masses and radii for PSR J0030+0451, and PSR J0740+6620 (68.3% credible interval) are inferred from NICER data, and the mass range extracted for the secondary of the GW190814 event is shown as well.

Multimessenger
astrophysics of
compact stars
with exotic
cores

A Sedrakian

Current
astrophysical
constraints

Introduction
and motivation

Current
astrophysical
constraints

Hyperons and
Delta-
resonances

Equation of
state of dense
matter

Results

Bulk viscosity
from direct
Urca processes

Results

Conclusions-II

Hyperons and delta-resonances and in proto-neutron stars and merger remnants

The equation of state (EoS) and composition of dense and hot Δ -resonance admixed hypernuclear matter is studied under conditions that are characteristic of neutron star binary merger remnants and supernovas.

- Baryon and lepton charges:

$$Y_Q = n_Q/n_B, \quad Y_{e,\mu} = (n_{e,\mu} - n_{e^+,\mu^+})/n_B$$

$$n_Q = n_p + n_{\Sigma^+} + 2n_{\Delta^{++}} + n_{\Delta^+} - (n_{\Sigma^-} + n_{\Xi^-} + n_{\Delta^-}).$$

- Trapped regime - fixed lepton numbers

$$Y_{L,e} = Y_e + Y_{\nu_e} \quad Y_{L,\mu} = Y_\mu + Y_{\nu_\mu},$$

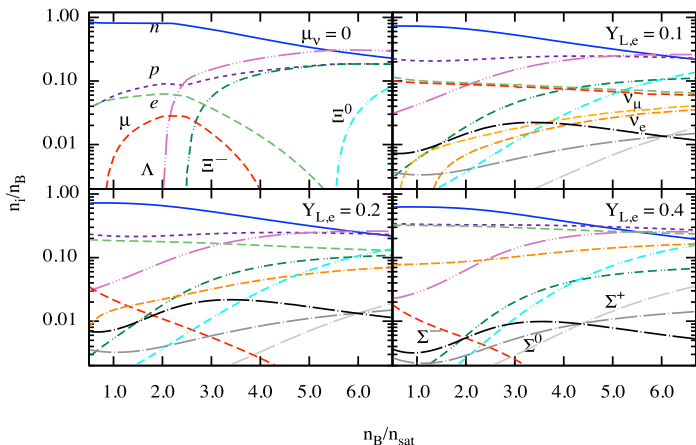
$$\text{BNS : } Y_{L,e} = Y_{L,\mu} = 0.1 \quad \text{Supernova : } Y_{L,e} = 0.4 \quad Y_{L,\mu} = 0.$$

- Transparent regime (neutrino chemical potentials vanish) - equilibrium with respect to the weak processes imply

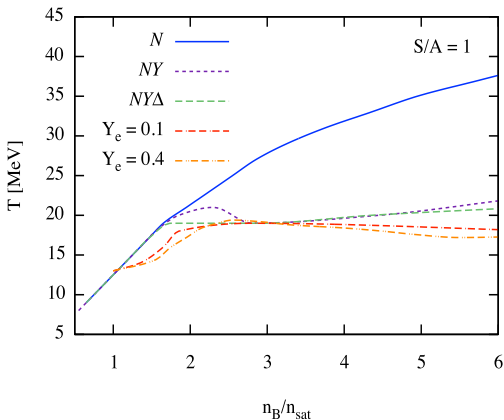
$$\mu_\Lambda = \mu_{\Sigma^0} = \mu_{\Xi^0} = \mu_{\Delta^0} = \mu_n = \mu_B, \quad \mu_{\Sigma^-} = \mu_{\Xi^-} = \mu_{\Delta^-} = \mu_B - \mu_Q,$$

$$\mu_{\Sigma^+} = \mu_{\Delta^+} = \mu_B + \mu_Q, \quad \mu_{\Delta^{++}} = \mu_B + 2\mu_Q,$$

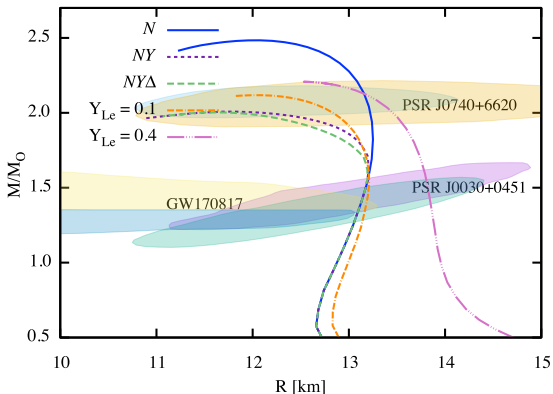
where the baryon μ_B and charge $\mu_Q = \mu_p - \mu_n$ chemical potentials are associated with conservations of these quantities.

Dependence of composition on baryon density for fixed T .

Dependence of the particle fractions n_i/n_B on the baryon density n_B normalized by the saturation density. The panels show the composition of $npe\mu$ matter in β -equilibrium at $T = 1$ MeV in the neutrino-free case ($\mu_\nu = 0$) and for neutrino-trapped matter at $T = 50$ MeV for several values of the electron lepton fraction $Y_{L,e} = 0.1, 0.2, 0.4$., with the μ -on component satisfying $Y_{L,\mu} = Y_{L,e} = 0.1$ and $Y_{L,\mu} = 0$ for $Y_{L,e} = 0.2, 0.4$, where $Y_{L,\mu}$ is the μ -on lepton fraction.

Dependence of temperature on density for fixed $S/A = 1$.

No significant changes in the composition compared to fixed T .



Gravitational mass versus radius for non-rotating spherically-symmetric stars. Three sequences are shown for β -equilibrated, neutrino-transparent stars with nucleonic (N), hypernuclear (NY) and Δ -admixed hypernuclear ($NY\Delta$) composition for $T = 0.1$ MeV. In addition, we show sequences of fixed $S/A = 1$ neutrino-trapped, isentropic stars composed of $NY\Delta$ matter in two cases of constant lepton fractions $Y_{Le} = Y_{L\mu} = 0.1$ and $Y_{Le} = 0.4$, $Y_{L\mu} = 0$. The ellipses show 90% CI regions for PSR J0030+0451, PSR J0740+6620 and gravitational wave event GW170817.

Multimessenger
astrophysics of
compact stars
with exotic
cores

A Sedrakian

Current
astrophysical
constraints

Introduction
and motivation

Current
astrophysical
constraints

Hyperons and
Delta-
resonances

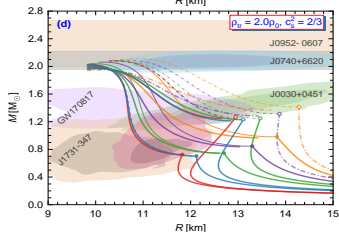
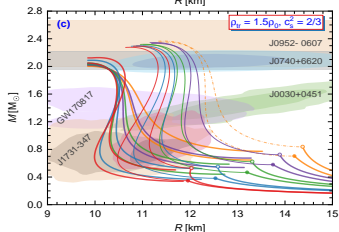
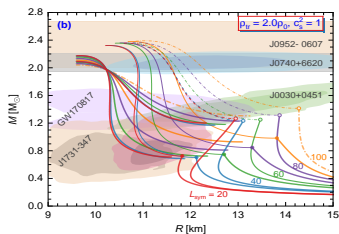
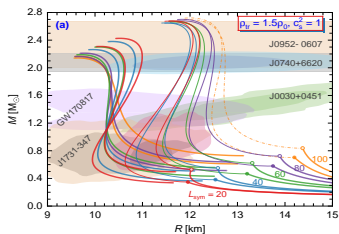
Equation of
state of dense
matter

Results

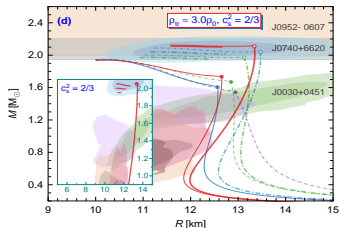
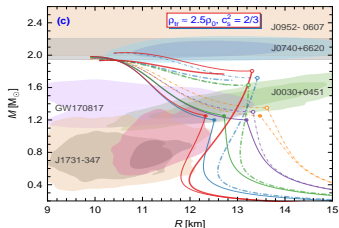
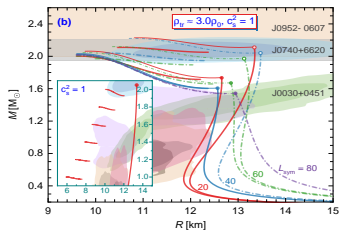
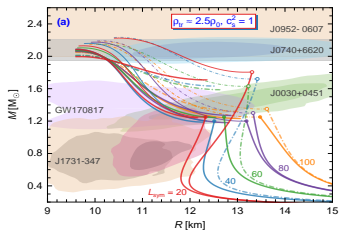
Bulk viscosity
from direct
Urca processes

Results

Conclusions-II



Mass-radius relations for hybrid EoS with $\rho_{tr} = 1.5 \rho_0$ and $2.0 \rho_0$, for $c_s^2 = 1$ and $2/3$ in the quark phase. In each panel, the hybrid EoS are built upon nucleonic models grouped by $L_{\text{sym}} = 20, 40, 60, 80$ and 100 MeV; for each, Q_{sat} is set to -600 and 1000 MeV. Solid lines represent models that satisfy all constraints, while dash-dotted lines show those failing for J1731-347. For each nucleonic EoS, thick lines show the hybrid models with a maximum energy jump that yields twin configurations and a branch passing through the 95% confidence region for the mass-radius constraints for PSR J0740+6620 and J0030+0451. [arXiv:2401.02198]



Mass-radius relations for hybrid EoSs with $\rho_{\text{tr}} = 1.5\rho_0$ and $2.0\rho_0$, for $c_s^2 = 1$ and $2/3$ in the quark phase. In each panel, the hybrid EoSs are built upon nucleonic models grouped by $L_{\text{sym}} = 20, 40, 60, 80$ and 100 MeV; for each, Q_{sat} is set to -600 and 1000 MeV. The circle on each curve denotes the configuration with central density ρ_{tr} ; lines ending with a filled circle are for the isoscalar-soft nucleonic model with $Q_{\text{sat}} = -600$ MeV and lines ending with an empty circle are for the isoscalar-stiff one with $Q_{\text{sat}} = 1000$ MeV. The thin lines show the model with a critical value of $\Delta\epsilon$ for which a higher value leads to a disconnected mass-radius curve. [arXiv:2401.02198]

Multimessenger
astrophysics of
compact stars
with exotic
cores

A Sedrakian

Current
astrophysical
constraints

Introduction
and motivation

Current
astrophysical
constraints

Hyperons and
Delta-
resonances

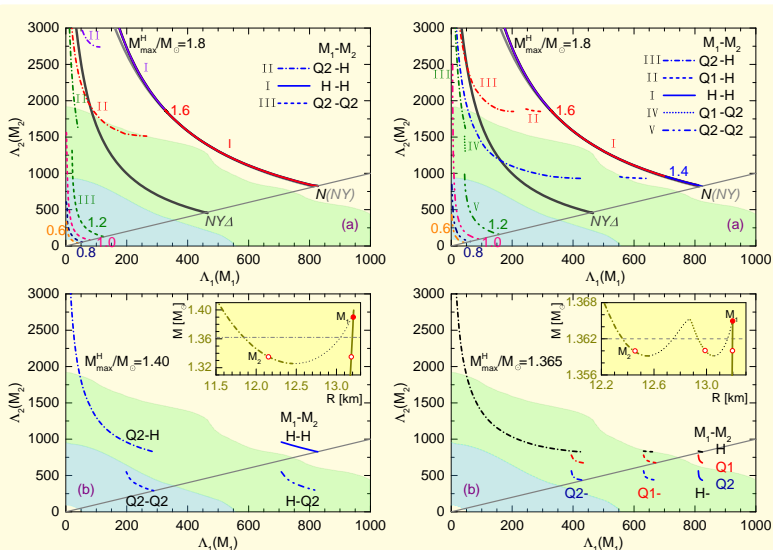
Equation of
state of dense
matter

Results

Bulk viscosity
from direct
Urca processes

Results

Conclusions-II



Tidal deformabilities of compact objects with single (left) and double (right) phase transition(s) for a fixed value of binary chirp mass $\mathcal{M} = 1.186 M_\odot$.

Urca rates including muons and leptonic processes

Bulk viscosity of moderately hot and dense, neutrino-transparent relativistic nucleonic matter arising from weak interaction is the dominant dissipative process in binary neutron star mergers.

Direct Urca reactions:

$$n \rightleftharpoons p + e^{-} + \bar{\nu}_e \quad (\text{neutron } e^{-} \text{ - decay}),$$

$$p + e^{-} \rightleftharpoons n + \nu_e \quad (\text{electron capture}),$$

$$n \rightleftharpoons p + \mu^{-} + \bar{\nu}_\mu \quad (\text{neutron } \mu^{-} \text{ - decay}),$$

$$p + \mu^{-} \rightleftharpoons n + \nu_\mu \quad (\text{muon capture}).$$

Leptonic reactions:

$$\mu \rightleftharpoons e^{-} + \bar{\nu}_e + \nu_\mu \quad (\text{muon decay}),$$

$$\mu + \nu_e \rightleftharpoons e^{-} + \nu_\mu \quad (\text{neutrino scattering}),$$

$$\mu + \bar{\nu}_\mu \rightleftharpoons e^{-} + \bar{\nu}_e \quad (\text{antineutrino scattering}).$$

Density oscillations in neutron-star matter

Consider now small-amplitude density oscillations in baryonic matter with frequency ω

$$n_j(t) = n_{j0} + \delta n_j(t), \quad \delta n_j(t) = \delta n_j^{\text{eq}}(t) + \delta n_j'(t), \quad j = \{n, p, e, \nu\},$$

The oscillations cause perturbations in particle densities due to which the chemical equilibrium of matter is disturbed leading to a small shift which can be written as

$$\mu_\Delta(t) = A_n \delta n_n(t) + A_\nu \delta n_\nu(t) - A_p \delta n_p(t) - A_e \delta n_e(t), \quad A_{ij} = \frac{\partial \mu_i}{\partial n_j}.$$

Out of equilibrium the chemical equilibration rate to linear order in $\mu_\Delta(t)$ is given by

$$\Gamma_\Delta \equiv \Gamma_p - \Gamma_n = \lambda \mu_\Delta, \quad \lambda > 0,$$

The β -equilibration rate (for example) is

$$\begin{aligned} \Gamma_{n \rightarrow p \bar{\nu}} &= \int \frac{d^3 p}{(2\pi)^3 2p_0} \int \frac{d^3 p'}{(2\pi)^3 2p'_0} \int \frac{d^3 k}{(2\pi)^3 2k_0} \int \frac{d^3 k'}{(2\pi)^3 2k'_0} \sum |\mathcal{M}_{\text{Urca}}|^2 \\ &\times \bar{f}(k) \bar{f}(p) \bar{f}(k') f(p') (2\pi)^4 \delta^{(4)}(k + p + k' - p'). \end{aligned} \quad (3)$$

(4)

Bulk viscosity

The rate equations which take into account the loss and gain of particles read as

$$\frac{\partial}{\partial t} \delta n_n(t) = -\theta n_{n0} - \lambda \mu_{\Delta}(t), \quad \dots \quad (5)$$

$\theta = \partial_i v_i$ is the fluid velocity divergence.

The non-equilibrium part of the pressure:

$$\Pi = \sum_j \frac{\partial p}{\partial n_j} \delta n'_j = -\zeta \theta, \quad \boxed{\zeta = \frac{C^2}{\sum_j A_j} \frac{\gamma}{\omega^2 + \gamma^2}}. \quad (6)$$

where

$$\gamma = \lambda \sum_j A_j, \quad C = n_{n0} A_n + n_{\nu 0} A_{\nu} - n_{p0} A_p - n_{e0} A_e = n_B \left(\frac{\partial \mu_{\Delta}}{\partial n_B} \right)_{Y_n}$$

Damping time-scale

The energy dissipation rate by the bulk viscosity per unit volume is

$$\frac{d\epsilon}{dt} = \frac{\omega^2 \zeta}{2} \left(\frac{\delta n_B}{n_B} \right)^2.$$

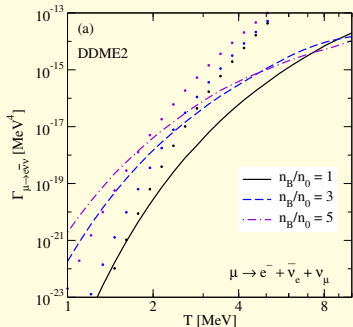
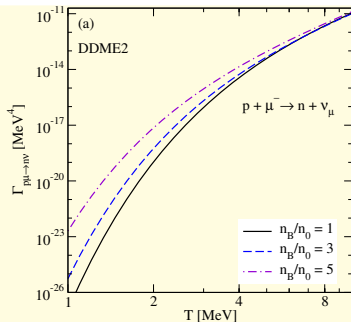
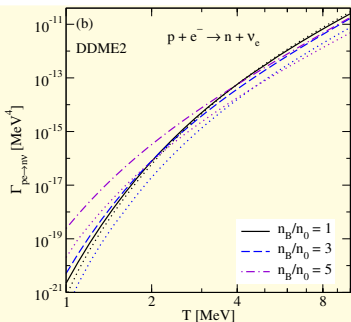
The characteristic timescale required for damping of oscillations

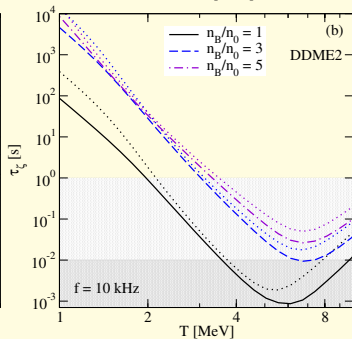
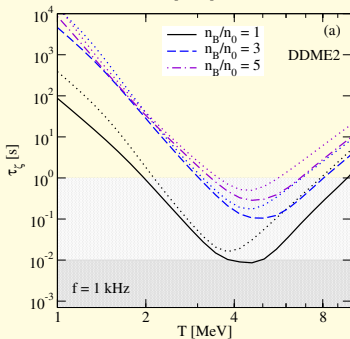
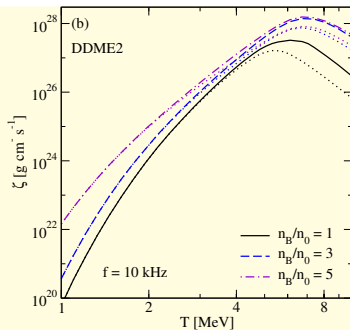
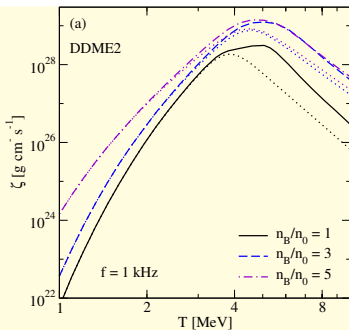
$$\tau_\zeta = \epsilon \left(\frac{d\epsilon}{dt} \right)^{-1} = \frac{1}{9} \frac{Kn_B}{\omega^2 \zeta}.$$

The minimal/maximal value of the damping timescale is

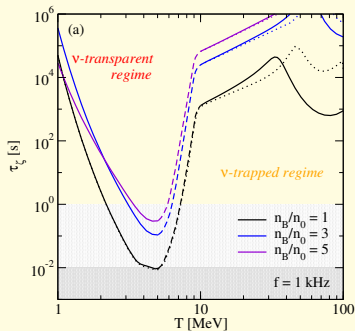
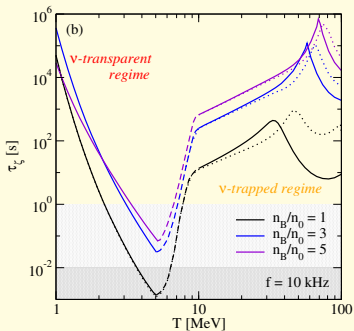
$$\tau_\zeta^{\min} = \frac{2}{9\omega} \frac{Kn_B}{C^2/A}, \quad \tau_\zeta^{\text{slow}} = \frac{1}{9\gamma} \frac{Kn_B}{C^2/A}, \quad \tau_\zeta^{\text{fast}} = \frac{\gamma}{9\omega^2} \frac{Kn_B}{C^2/A}.$$

In the limits of slow and fast equilibration the damping timescale is given by





Combined neutrino transparent and trapped regimes:



The shaded regions show where the damping timescale becomes smaller than the short-term ($\simeq 10$ ms, dark shaded areas) and long-term ($\simeq 1$ s, light shaded areas) evolution timescales of a BNS merger remnant object. For a typical oscillation frequency $f = 1$ kHz, bulk viscous damping would be marginally relevant in the short term, and noticeable for long-living remnants ms at any density and in the temperature range $2 \leq T \leq 10$ MeV.

Physics output, conclusions and future:

- Constructed relativistic density functionals which are best constrained by current laboratory and astrophysical data. Flexible parameterizations allow for the exploration of parameter space.
- Created a large number of stellar models for injection studies of the Einstein Telescope (mass, radius, tidal deformabilities, variation of characteristics L and Q of the EoS).
- 2D EoS tables can be downloaded from, J.-J. Li and A. Sedrakian, Ap. J. 957:41 (2023) https://github.com/asdrakian/DD_CDFs/ repository.
- Worked out finite temperature analogs of EoS and 3D tables for numerical simulations, S. Tsiopelas, A. Sedrakian, M. Oertel (TSO), Eur. Phys. J. A (2024) 60:127
- 3D EoS tables can be downloaded from <https://compose.obspm.fr/eos/321>
- More on properties of hot compact stars: rotation, universal relation, arXiv:2306.14190, arXiv:2102.00988, arXiv:2008.00213.
- Exotic cores of compact stars offer interesting physics whose generic features have been determined independent of particular models.
- In the future we need an integrated approach where EoS and transport will be bundled together to provide a consistent microscopic framework for numerical experiments and physical studies of compact stars.

Multimessenger
astrophysics of
compact stars
with exotic
cores

A Sedrakian

Current
astrophysical
constraints

Introduction
and motivation

Current
astrophysical
constraints

Hyperons and
Delta-
resonances

Equation of
state of dense
matter

Results

Bulk viscosity
from direct
Urca processes

Results

Conclusions-II

Journals / Particles



Submit to Particles

Review for Particles



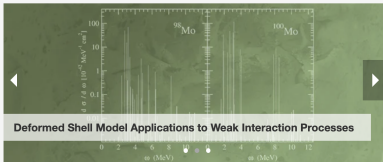
Share

Journal Menu

- [Particles Home](#)
- [Aims & Scope](#)
- [Editorial Board](#)
- [Reviewer Board](#)
- [Instructions for Authors](#)
- [Special Issues](#)
- [Topical Collections](#)
- [Article Processing Charge](#)
- [Indexing & Archiving](#)
- [Editor's Choice Articles](#)
- [Most Cited & Viewed](#)
- [Journal Statistics](#)
- [Journal History](#)
- [Journal Awards](#)
- [Editorial Office](#)

Journal Browser

<https://www.mdpi.com/journal/particles#> auf dieser Seite in einem neuen Tab öffnen



Particles

Particles is an international, open access, peer-reviewed journal covering all aspects of nuclear physics, particle physics and astrophysics science, and is published quarterly online by MDPI.

- **Open Access** — free for readers, with article processing charges (APC) paid by authors or their institutions.
- **High Visibility:** indexed within Scopus, ESCI (Web of Science), Inspec, CAPIUS / SciFinder, and other databases.
- **Journal Rank:** JCR - Q2 (Physics, Nuclear) / CiteScore - Q2 (Physics and Astronomy (miscellaneous))
- **Rapid Publication:** manuscripts are peer-reviewed and a first decision is provided to authors approximately 27.4 days after submission; acceptance to publication is undertaken in 3.8 days (median values for papers published in this journal in the first half of 2024).
- **Recognition of Reviewers:** reviewers who provide timely, thorough peer-review reports receive vouchers entitling them to a discount on the APC of their next publication in any MDPI journal, in appreciation of the work done.

IMPACT
FACTOR
1.7

CITESCORE
3.2

E-Mail Alert

Add your e-mail address to receive forthcoming issues of this journal:

News

19 August 2024

**MDPI's 2023 Young Investigator Awards
— Winners Announced**



2023 Young
Investigator
Award Winners



2 August 2024

**MDPI Romania Author Training
Sessions in May**

10 July 2024

**MDPI's Newly Launched Journals in
June 2024**